Bioorganic & Medicinal Chemistry Letters 19 (2009) 2053–2058

Contents lists available at ScienceDirect

Bioorganic & Medicinal Chemistry Letters

journal homepage: www.elsevier.com/locate/bmcl

Exploring the pharmacokinetic properties of phosphorus-containing selective HDAC 1 and 2 inhibitors (SHI-1:2)

Richard W. Heidebrecht Jr.[a,*], Melissa Chenard[c], Joshua Close[a], William K. Dahlberg[a], Judith Fleming[b], Jonathan B. Grimm[a], Julie E. Hamill[a], Andreas Harsch[a], Brian B. Haines[c], Bethany Hughes[a], Astrid M. Kral[b], Richard E. Middleton[a], Chandrasekhar Mushti[a], Nicole Ozerova[b], Alexander A. Szewczak[a], Hongmei Wang[b], Kevin Wilson[a], David J. Witter[a], J. Paul Secrist[b], Thomas A. Miller[a]

[a] Department of Drug Design and Optimization, Merck Research Laboratories, 33 Avenue Louis Pasteur, Boston, MA 02115, USA
[b] Department of Cancer Biology and Therapeutics, Merck Research Laboratories, 33 Avenue Louis Pasteur, Boston, MA 02115, USA
[c] Department of Oncology Pharmacology, Merck Research Laboratories, 33 Avenue Louis Pasteur, Boston, MA 02115, USA

ARTICLE INFO

Article history:
Received 3 December 2008
Revised 2 February 2009
Accepted 3 February 2009
Available online 8 February 2009

Keywords:
Pharmacokinetics
Selective histone deacetylase inhibitor
Zolinza
Xenograft
Phosphorus-containing therapeutic

ABSTRACT

We report the preparation and structure–activity relationships of phosphorus-containing histone deacetylase inhibitors. A strong trend between decreasing phosphorus functional group size and superior mouse pharmacokinetic properties was identified. In addition, optimized candidates showed tumor growth inhibition in xenograft studies.

The control of gene expression is maintained by direct chemical modifications to DNA and control of chromatin structure. The 'histone code' of chromatin is represented by differential methylation of lysine and arginine residues combined with acetylation state of lysine residues on the four types of histones (H1–H4). These epigenetic signals, combined with DNA modifications such as CpG island methylation, represent a complex and tunable mechanism for gene expression. Analogous to mutations of the primary structure of DNA, aberrant epigenetic changes have been linked to a growing number of human diseases, including cancer.[1]

Histone deacetylases (HDACs), in combination with histone acetylases (HATs), are important regulators of epigenetic equilibrium.[2] The eleven known zinc-dependent HDACs are divided into three classes based on sequence homology. Class I enzymes (HDACs 1–3, 8) are predominantly found in the nucleus and consist of 350–500 amino acid residues, while class II examples (HDACs 4–7, 9–10) are tissue specific, shuttle between the cytoplasm and the nucleus, and are about 1000 amino acids in length. The single member of the class III HDACs (HDAC 11) contains two active sites, and displays characteristics of both class I and II enzymes. The complex underlying biology of HDACs, combined with the first clinically successful inhibitor Zolinza®, makes understanding the systematic modification of the action of these enzymes an important field in medicinal chemistry.

Zolinza® became the first HDAC inhibitor to gain approval in the United States, and is indicated for the treatment of cutaneous manifestations of cutaneous T-cell lymphoma (Fig. 1).[3] In the *ortho*-amino benzamide class of HDAC inhibitor, MS-275 has entered clinical trials for several oncological indications.[4] Another example

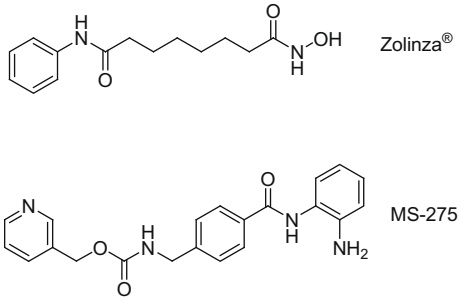

Figure 1. HDAC inhibitors Zolinza® and MS-275.

* Corresponding author.
E-mail address: richard_heidebrecht@merck.com (R.W. Heidebrecht Jr.).

0960-894X/$ - see front matter © 2009 Elsevier Ltd. All rights reserved.
doi:10.1016/j.bmcl.2009.02.009

from this class is **1**, a potent *ortho*-amino benzamide malonate developed in our laboratory with a structurally distinct surface recognition domain.[5] Our most recent reports are exemplified by biphenyl SHI-1:2 **2** (Fig. 2),[6] which projects an aryl ring into the internal cavity of HDACs 1 and 2 (putatively not accommodated by other HDAC's), resulting in excellent selectivity over the HDAC3 isoform.[7]

As exemplified by the inhibitors above (Figs. 1 and 2), we looked to further expand our understanding of moieties that optimize interactions at the surface recognition domain.[8] It has been noted that phosphonates and malonates can be bioisosteric.[9] With this in mind, we pursued the synthesis of derivatives containing both phosphorus-based functional groups in the surface recognition domain and a biphenyl warhead to facilitate HDAC 1:2 selectivity.

Our initial synthetic efforts were directed toward simple aryl and benzylically oriented phosphorus-containing inhibitors. The aryl examples were prepared via nickel-catalyzed cross coupling (Scheme 1). A combination of methyl 4-bromobenzoate (**3**), a phosphonite ($PR(OR)_2$), and catalytic nickel(II) bromide was heated at elevated temperatures without solvent to afford phosphinate **4**.[10] Saponification, amide formation, and deprotection led to our target compounds **6**. Phosphonate **6a** (R^1, R^2 = OEt) was prepared via a truncated route from the corresponding commercially available substituted benzoate.[11]

While many of the phosphonites ($PR(OR)_2$) and phosphinites ($PR_2(OR)$) required to prepare the requisite derivatives were commercially available, the remainder were prepared via displacement of the corresponding chloride (Scheme 2). Reactants required for cross-couplings (e.g., Scheme 1) were prepared in pentane, filtered, and concentrated.[12] Those designated for benzylic derivatives (e.g., Scheme 3) were synthesized in toluene, filtered to remove amine salts, and directly used in subsequent reactions.

The benzylic examples (e.g., Scheme 3) were prepared via a Michaelis-Arbuzov approach.[13] Bromomethylbenzoyl bromide **8** was treated with monoprotected diamine **7** to afford amide **9** (Scheme 3). This key intermediate (**9**) was reacted with a range of phosphites, phosphonites, and phosphinites to afford, after deprotection, target compounds **11**.

The phosphonic and phosphinic acid derivatives were prepared via hydrolysis of the corresponding methoxy and ethoxy phosphonates and phosphinates with NaOH in dioxane at elevated temperatures.[14] This reaction was performed on the deprotected compounds, affording **6b** and **11b**/**f** wherein R^2 = OH.

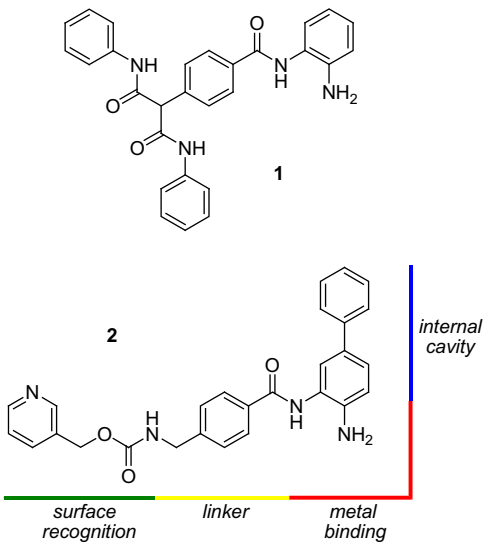

Figure 2. HDAC inhibitors **1** and **2** superimposed with the pharmocophore.

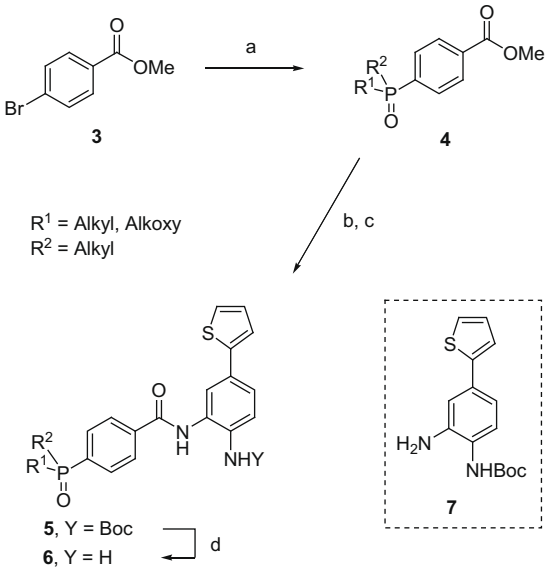

Scheme 1. The synthesis of aryl phosphorus derivatives **6a**, **c**, **d**, **e**, and **f**. Reagents and conditions: (a) $NiBr_2$, phosphonite ($RP(OR)_2$), 160 °C, neat; (b) LiOH, THF/MeOH/water; (c) **7**, EDC, DMF; (d) TFA, DCM.

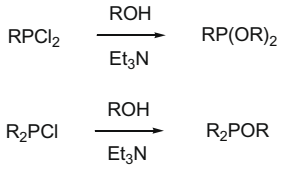

Scheme 2. The preparation of phosphonites ($PR(OR)_2$) and phosphinites $P(R)_2(OR)$.

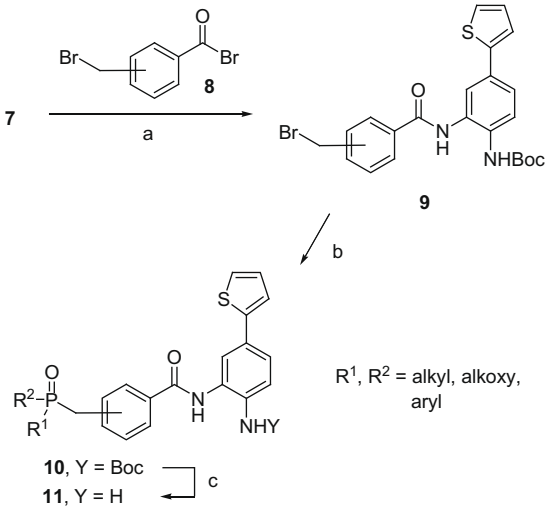

Scheme 3. The synthesis of benzylic phosphorus derivatives **11a**, **c**, **e**, **g**–**k**, **m**–**p**. Reagents and conditions: (a) **8**, iPr_2NEt, DCM; (b) phosphite ($P(OR)_3$), phosphonite ($RP(OR)_2$), or phosphinite ($(R)_2POR$), toluene, Δ; (c) TFA, DCM.

To facilitate late-stage generation of structural diversity, a sequence was developed beginning with protected benzylically-oriented intermediate **10** (Scheme 4). Methoxy-substituted phosphonates and phosphinates (**10**) were hydrolyzed, and their corresponding acids were subjected to BOP[15] coupling; deprotection provided target compounds **11**.

Other structurally unique examples were prepared during the course of this work. For example, amino phosphonate **13** proved

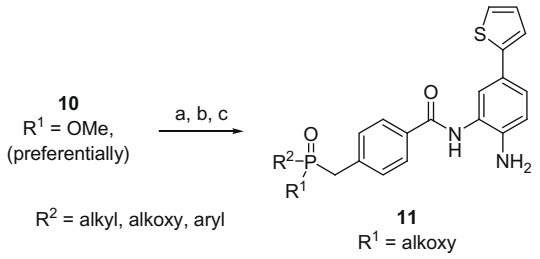

Scheme 4. The synthesis of phosphonate and phosphinate ester libraries, including compound **11l**. Reagents and conditions: (a) NaOH, dioxane, Δ; (b) Alcohol R^1OH, BOP, iPr_2NEt, DMF; (c) TFA, DCM.

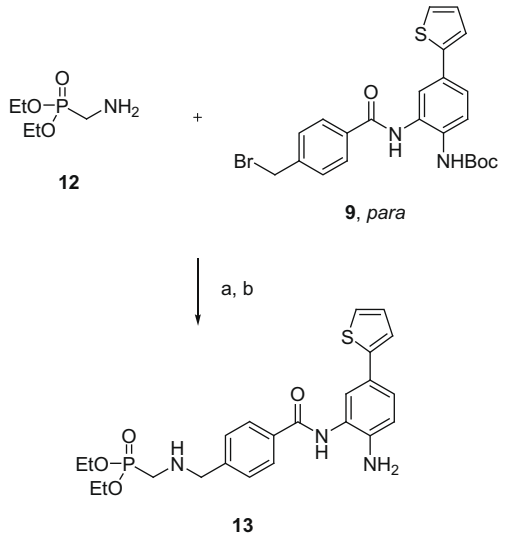

Scheme 5. The synthesis of aminophosphonate **13**. Reagents and conditions: (a) iPr_2NEt, DMF, 50 °C; (b) TFA, DCM.

to be particularly promising; its synthesis is depicted in Scheme 5. Key benzyl bromide **9** (4-substituted) was treated with diethyl (aminomethyl) phosphonate (**12**)[16] and deprotected to afford target **13** (Scheme 5).

Gratifyingly, HDAC inhibitors with a phosphorus-based surface recognition element generally led to compounds with in vitro activity in the low nanomolar range (Table 1). Both aryl and benzylically-substituted examples were potent inhibitors of HDAC1 enzyme and proliferation in HDAC-dependent HCT116 cells[17] across three phosphorus oxidation states: phosphonates, phosphinates, and phosphine oxides.

Para-substituted benzamides were generally more potent inhibitors of cell proliferation than their analogous *meta* examples with corresponding differences in measured GI_{50} values; compare examples **11a** and **11c** (GI_{50} = 0.250, 2.50 μM, respectively), **11e** and **11g** (GI_{50} = 0.360, 8.60 μM, respectively), **11h** and **11i** (GI_{50} = 0.130, 6.00 μM, respectively), **11j** and **11k** (GI_{50} = 0.200, >20.0 μM, respectively). It was also apparent that the acids of both phosphonates (**6b**, HDAC1 IC_{50} = 42nM and **11b**, HDAC1 IC_{50} = 38 nM) and phosphinates (**11f**, HDAC1 IC_{50} = 38 nM) were potent in the cell free enzyme assay but were not effective in the inhibition of immortalized cell growth (GI_{50} > 20 μM), presumably due to lack of cell permeability.

It should be noted that several examples were prepared that varied the biphenyl aryl ring. Similar properties were observed between phenyl, 2-thiophene, and 3-thiophene substituents.[18] The 2-thiophene 'warhead' was utilized due to a general trend affording modest advantages in GI_{50} in HCT-116 cells.

With a range of potent compounds in hand, we turned to evaluate our leads in pharmacokinetic (PK) and pharmacokinetic/pharmacodynamic (PK/PD) assays. Compound **11a** demonstrated promising PK in the rat, possessing relatively low plasma clearance (Cl_p = 15.8 mL/min/kg) and acceptable oral bioavailability and exposure (F = 45%, P.O. $AUC_{(0-\infty)}$ = 4.40 μM h). These results prompted us to assess the acetylation state of H2B histones after dosing of HCT116 tumor-bearing nude CD-1 mice at 150 mg/kg qd for three days. Compound **2** was used as a positive control. Unfortunately, initial lead **11a** did not show a significant increase in acetylation relative to vehicle (Fig. 3).[19] This can be explained by the low exposure of **11a** achieved after ip administration (1.54 μM in plasma, 3 h post-dose), suggesting that the compound had high clearance in mice. The pharmacokinetics of **11a** in mouse and dog were assessed, revealing clearance greater than hepatic blood flow in both species.

A significant improvement in mouse PK was required in order to determine the in vivo potency and efficacy of our phosphorus-

Table 1
Exploration of phosphorus-based functional groups

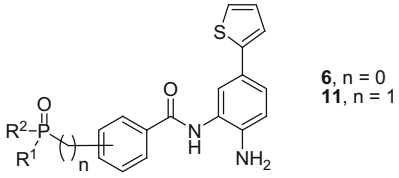

	Compound	*n*	Substitution	R^1	R^2	HDAC1 IC_{50} (nM)	GI_{50} HCT116 (μM)
Phosphonates	**6a**	0	4	OEt	OEt	22	0.410
	6b	0	4	OEt	OH	42	>20
	11a	1	4	OEt	OEt	13	0.250
	11b	1	4	OEt	OH	38	>20
	11c	1	3	OEt	OEt	23	2.5
Phosphonites	**6c**	0	4	OEt	Me	14	0.46
	6d	0	4	OMe	Ph	29	0.38
	11e	1	4	OMe	Ph	20	0.36
	11f	1	4	OH	Ph	28	>20
	11g	1	3	OMe	Ph	140	8.6
	11h	1	4	OMe	Et	7	0.130
	11i	1	3	OMe	Et	90	6.0
Phosphine oxides	**11j**	1	4	Et	Et	9	0.20
	11k	1	3	Et	Et	270	>20

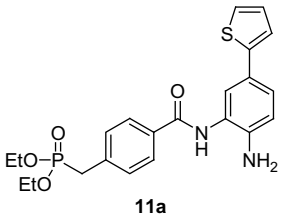

11a

HDAC1 IC_{50}: 13 nM
HCT116 GI_{50}: 250 nM

PK/PD$_{(mouse)}$: negative

Rat (Sprague-Dawley)
AUC: 4.40 μM h
Cl: 15.8 mL/min/Kg
Vd_{ss}: 7.27 L/kg
$t_{1/2}$: 5.5h

Mouse (Swiss-Webster)
AUC: 0.17 μM h
Cl: >Hept
Vd_{ss}: 20.1 L/kg
$t_{1/2}$: 55 h

Dog (Beagle)
AUC: 0.25 μM h
Cl: >Hept
Vd_{ss}: 2.85 L/kg
$t_{1/2}$: 0.43 h

Figure 3. Summary of data for compound **11a**.

based inhibitors. A streamlined assay to facilitate the weekly assessment of oral exposure of compounds in mice was designed. New chemical entities were dosed orally at 150 mg/kg, and measurements were taken from whole blood collected by nicking the tail vein at six time points from 0.25 h to 7 h.

An analysis of the mouse pharmacokinetic data from phosphorus-containing inhibitors indicated a strong trend where smaller substituents led to compounds with superior exposure (Table 2). In the analogs where there is an aryl-phosphorus bond (**6e–6f**), going from a phenyl/ethoxy substitution (**6e**, AUC = 0.91 μM h) to a methyl/ethoxy phosphinate (**6c**, AUC = 44 μM h) resulted in a marked improvement in maximum exposure. These aryl examples did not appear particularly sensitive to the identity of the alkoxy groups, exemplified by a small difference between methoxy (**6f**, AUC = 60 μM h) and ethoxy (**6c**, AUC = 44 μM h) phosphinates when the alkyl group remained constant (Me).

The benzylically-substituted phosphinate examples demonstrated a similar effect (Table 2, **11l–11o**). The largest effect was observed on the alkoxy group of these phosphinates. As the alkyl group is held as a methyl, a constant and remarkable improvement in exposure is observed when going from larger phosphinate esters such as 3-pyridylmethyl analog **11l** (AUC = 16 μM h) to ethoxy

Table 2
The critical relationship between the groups on phosphorus and mouse PK parameters

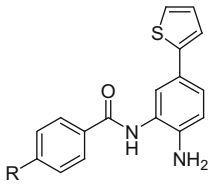

Compound	R	HDAC1 IC_{50} (nM)	GI_{50} HCT116(μM)	C_{max} (μM)	AUC (μM h)
6e		21	0.170	0.56	0.91
6d		29	0.380	11	12
6c		14	0.460	43	44
6f		52	0.420	39	60
11l	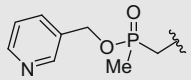	3.5	0.130	8.8	16
11m	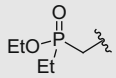	6.5	0.240	17	17
11n	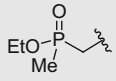	16	0.330	31	50
11o	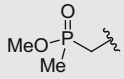	54	0.160	88	115
11p	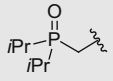	11	0.270	1.9	1.3
11j	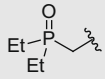	8.5	0.200	14	17

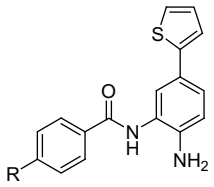

Compound	R	Data Summary
11n	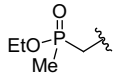	HDAC1 IC_{50}: 16 nM HCT116 GI_{50}: 0.330 μM $PD_{(mouse)}$: negative Time Post Dose (h): 24
11o	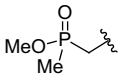	HDAC1 IC_{50}: 54 nM HCT116 GI_{50}: 0.160 μM $PD_{(mouse)}$: positive Time Post Dose (h): 24
13	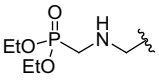	HDAC1 IC_{50}: 7.7 nM HCT116 GI_{50}: 0.300 μM $PD_{(mouse)}$: positive Time Post Dose (h): 8

Figure 4. Summary of data for compounds **11n**, **11o**, and **13**.

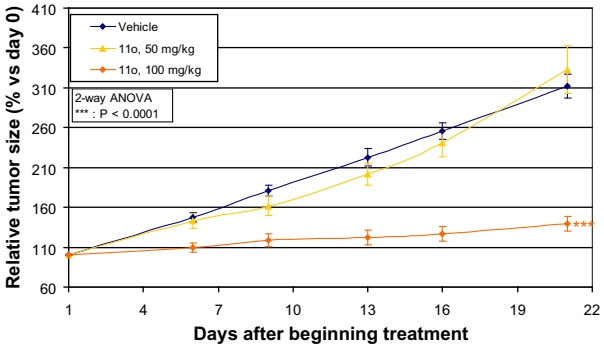

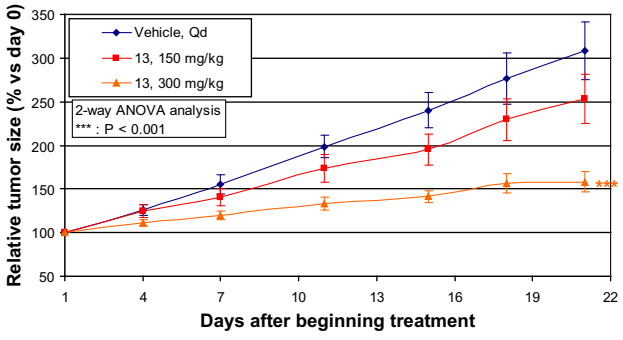

Figure 5. Xenograft results for compounds **11o** and **13**.

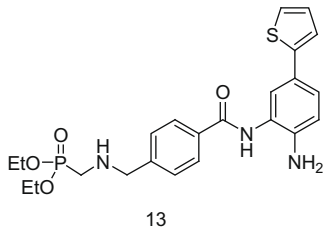

13

HDAC1 IC_{50}:	7.7 nM
HDAC2 IC_{50}:	14 nM
HDAC3 IC_{50}:	12000 nM
HDAC4 IC_{50}:	>50000 nM
HDAC5 IC_{50}:	>50000 nM
HDAC6 IC_{50}:	>50000 nM
HDAC7 IC_{50}:	>50000 nM
HDAC8 IC_{50}:	37000 nM
HDAC11 IC_{50}:	>50000 nM

Figure 6. Full HDAC selectivity data for **13**.

compound **11n** (AUC = 50 μM h). The most dramatic result was obtained with methoxy example **11o** (AUC = 115 μM h).

Minor improvements in AUC were observed when smaller phosphorus-linked alkyl groups were installed. This is exemplified by a comparison of ethyl-substituted phosphinate **11m** (AUC = 17 μM h) with the closely related methyl derivative **11n** (AUC = 50 μM h). The same trend was observed for phosphine oxides: 4-diisopropyl-phosphinomethyl (AUC = 1.3 μM h) **11p** gave much reduced exposure compared to 4-diethylphosphinomethyl **11j** (AUC = 17 μM h).

Promising compounds were tested in the PK/PD model for histone acetylation (HCT116 tumor-bearing nude CD-1 mice, 150 mg/kg, po, qd, 3 days), and three examples are depicted below (Fig. 4). Phosphinate **11n** did not demonstrate changes to the ratio of acetylated to deacetylated H2B histones relative to control; however, a statistically significant response was demonstrated by both phosphinate **11o** and aminophosphonate **13**.

Leads **11o** and **13** were further tested in a mouse xenograft model (HCT116 colon) at various daily oral doses for 21 days (Fig. 5), and dose-dependent inhibition of tumor growth was observed. Unfortunately, mice treated with **11o** also experienced significant and dose proportionate weight loss (22% loss in the 100 mg/kg cohort after 21 days), affording a very small therapeutic window. On the other hand, compound **13** was very well tolerated at all doses, illustrating the potential utility of phosphorus based HDAC inhibitors for the treatment of cancer.

The phosphorus-containing biphenyl inhibitors disclosed in this work possess the excellent selectivity for HDACs 1 and 2 that was previously observed.[7b] Full data for compound **13** is provided as an example (Fig. 6).[20] A minimum of three logs of selectivity separates the in vitro HDAC1 (IC_{50} = 7.7 nM) and HDAC2 (IC_{50} = 14 nM) potency of **13** from other class I isoforms, i.e., the closely related HDAC3 (IC_{50} = 12,000 nM) as well as HDAC8 (IC_{50} = 37,000 nM). Excellent selectivity was observed over class II and III enzymes (HDACs 4–7, 11, IC_{50} = >50,000 nM).

In summary, we observed a disconnect between rat and mouse pharmacokinetics of phosphorus-containing SHI-1:2 analogs. A survey of mouse PK parameters showed a strong correlation between smaller alkyl phosphorus-based groups and superior oral exposure. Sample compound (**13**) showed promising and significant tumor growth inhibition in a xenograft model without significant weight loss.[21]

Acknowledgements

We would like to express our appreciation to Sujal Deshmukh and Dapeng Chen for assistance with pharmacokinetic studies.

References and notes

1. (a) Feinberg, A. P.; Vogelstein, B. *Nature* **1983**, *301*, 89; (b) Holliday, R. *Science* **1987**, *238*, 163; (c) Jones, P. A.; Baylin, S. B. *Nat. Rev. Genet.* **2002**, *3*, 415.
2. Grozinger, C. M.; Schreiber, S. L. *Chem. Biol.* **2002**, *9*, 3.
3. (a) Richon, V. M. *Br. J. Cancer* **2006**, *95*, S2; (b) O'Connor, O. A. *Br. J. Cancer* **2006**, *95*, S7; (c) Duvic, M.; Zhang, C. *Br. J. Cancer* **2006**, *95*, S13; (d) Marks, P. A.; Breslow, R. *Nat. Biotechnol.* **2007**, *25*, 84.
4. (a) Suzuki, T.; Ando, T.; Tsuchiya, K.; Fukazawa, N.; Saito, A.; Mariko, Y.; Yamashita, T.; Nakanishi, O. *J. Med. Chem.* **1999**, *42*, 3001; (b) Kell, J. *Curr. Opin. Invest. Drugs* **2007**, *8*, 485.
5. Siliphaivahn, P.; Harrington, P.; Witter, D. J.; Otte, K.; Tempest, P.; Katter, S.; Kral, A.; Fleming, J. C.; Deshmukh, S. V.; Harsch, A.; Secrist, P. J.; Miller, T. A. *Bioog. Med. Chem. Lett.* **2007**, *17*, 4619.
6. Moradei, O. M.; Mallais, T. C.; Frechette, S.; Paquin, I.; Tessier, P. E.; Leit, S. M.; Fournel, M.; Bonfils, C.; Trachy-Bourget, M.-C.; Liu, J.; Yan, T. P.; Lu, A.-H.; Rahil, J.; Wang, J.; Lefebvre, S.; Li, Z.; Vaisburg, A. F.; Besterman, J. M. *J. Med. Chem.* **2007**, *50*, 5543.
7. (a) Weerasinghe, S. V. W.; Estiu, G.; Wiest, O.; Pflum, M. K. *J. Med. Chem.* **2008**, *51*, 5542; (b) Witter, D. J.; Harrington, P.; Wilson, K. J.; Chenard, M.; Cruz, J. C.; Fleming, J. C.; Harsch, A.; Kral, A. M.; Secrist, J. P.; Miller, T. A. *Bioorg. Med. Chem. Lett.* **2008**, *18*, 726; (c) Methot, J. L.; Chenard, M. C.; Close, J.; Cruz, J. C.; Dahlberg, W. K.; Fleming, J.; Hamblett, C. L.; Hamill, J. E.; Harrington, O.;

Harsch, A.; Heidebrecht, R.; Hughes, B.; Jung, J.; Kenific, C. M.; Kral, A.; Middleton, R. E.; Ozerova, N.; Sloman, D. L.; Stanton, M. G.; Szewcrak, A.; Witter, D. J.; Secrist, J. P.; Miller, T. A. *Bioorg. Med. Chem. Lett.* **2008**, *18*, 973.

8. For the x-ray crystal structure of HDAC8 Finnin, M. S.; Donigian, J. R.; Cohen, A.; Richon, V. M.; Rifkind, R. A.; Marks, P. A.; Breslow, R.; Pavletich, N. P. *Nature* **1999**, *401*, 188. RCSB Protein Data Bank number 1C3S.
9. Gao, Y.; Luo, J.; Yao, Z.-J.; Guo, R.; Zou, H.; Kelley, J.; Voigt, J.; Yang, D.; Burke, R. R. *J. Med. Chem.* **2000**, *43*, 911.
10. Markl, G.; Gschwender, K.; Rotzer, I.; Kreitmeier, P. *Helv. Chim. Acta.* **2004**, *87*, 825.
11. Diethyl(4-carboxylphenyl)phosphonate, CAS 1527-34-0, ABCR, catalog number AB147504.
12. Denney, D. B.; Denney, D. Z.; Hammond, P. J.; Wang, Y.-P. *J. Am. Chem. Soc.* **1981**, *103*, 1785.
13. Bhattacharya, A. K.; Thyagarajan, G. *Chem. Rev.* **1981**, *81*, 415.
14. Methoxy-substituted examples saponified with superior results than the corresponding ethoxy examples, putatively as a result of the mechanism of alkaline hydrolysis. For a discussion of alkaline mechanism, see Cook, R. D.; Diebert, C. E.; Schwarz, W.; Turley, P. C.; Haake, P. *J. Am. Chem. Soc.* **1973**, *95*, 8088; Acidic hydrolysis is more facile, but incompatible with our BOC protecting group. For a discussion of acidic mechanism, see Abbas, K.; Cook, R. D. *Tetrahedron Lett.* **1975**, *41*, 3559.
15. 1*H*-Benzotriazol-1-yl-oxytris(dimethylamino) phosphonium hexofluorophoshate (BOP), CAS 056602-33-6. It is worth noting that the dehydration reaction yields inferior results with diimides such as EDC.
16. Commercially available from Acros Organics, CAS 117196-73-3. For a preparation, see Steere, J. A.; Sampson, P. B.; Honek, J. F. *Bioorg. Med. Chem. Lett.* **2002**, *12*, 457.
17. For assay details, see Ref. 7b.
18. For example, the 2-thienyl group in **6d** (HDAC1 IC_{50} = 29 nM, HCT-116 GI_{50} = 0.380 μM) was replaced with phenyl (HDAC1 IC_{50} = 19 nM, HCT-116 GI_{50} = 0.470 μM) and 3-thienyl (HDAC1 IC_{50} = 22 nM, HCT-116 GI_{50} = 0.460 μM) substituents.
19. Statistical significance was demonstrated via t-test analysis looking for a *P*-value of <0.05 relative to vehicle.
20. For assay details, see reference within Jones, P.; Altamura, S.; Chakravarty, P. K.; Cecchetti, O.; De Francesco, R.; Gallinari, P.; Ingenito, R.; Meinke, P. T.; Petrocchi, A.; Rowley, M.; Scarpelli, R.; Serafini, S.; Steinkühler, C. *Bioorg. Med. Chem. Lett.* **2006**, *16*, 5948.
21. The compounds described in this paper are the topic of a patent application. The reader is directed to this publication for experimental information: Close, J.; Grimm, J.; Heidebrecht, R. W.; Kattar, S.; Miller, T. A.; Otte, K. M.; Peterson, S.; Siliphaivanh, P.; Tempest, P.; Wilson, K. J.; Witter, D. J.; WO 2008010985.